Supporting Information

for

Insights into the Plasma-Assisted Fabrication and Nanoscopic Investigation of Tailored MnO_2 Nanomaterials

Davide Barreca,[‡]* *Filippo Gri,*[†] *Alberto Gasparotto,*[†] *Thomas Altantzis,*[§]

Valentina Gombac,[#] *Paolo Fornasiero,*[#] *and Chiara Maccato*[†]*

[‡] CNR-ICMATE and INSTM, Department of Chemical Sciences, Padova University, 35131 Padova, Italy.

[†] Department of Chemical Sciences, Padova University and INSTM, 35131 Padova, Italy.

[§] EMAT, University of Antwerp, 2020 Antwerp, Belgium.

[#] Department of Chemical and Pharmaceutical Sciences, ICCOM-CNR and INSTM, Trieste University, 34127 Trieste, Italy.

* Authors to whom correspondence should be addressed; E-mail: davide.barreca@unipd.it; chiara.maccato@unipd.it.

§ S-1. Characterization

§ S-1.1 X-ray photoelectron spectroscopy (XPS)

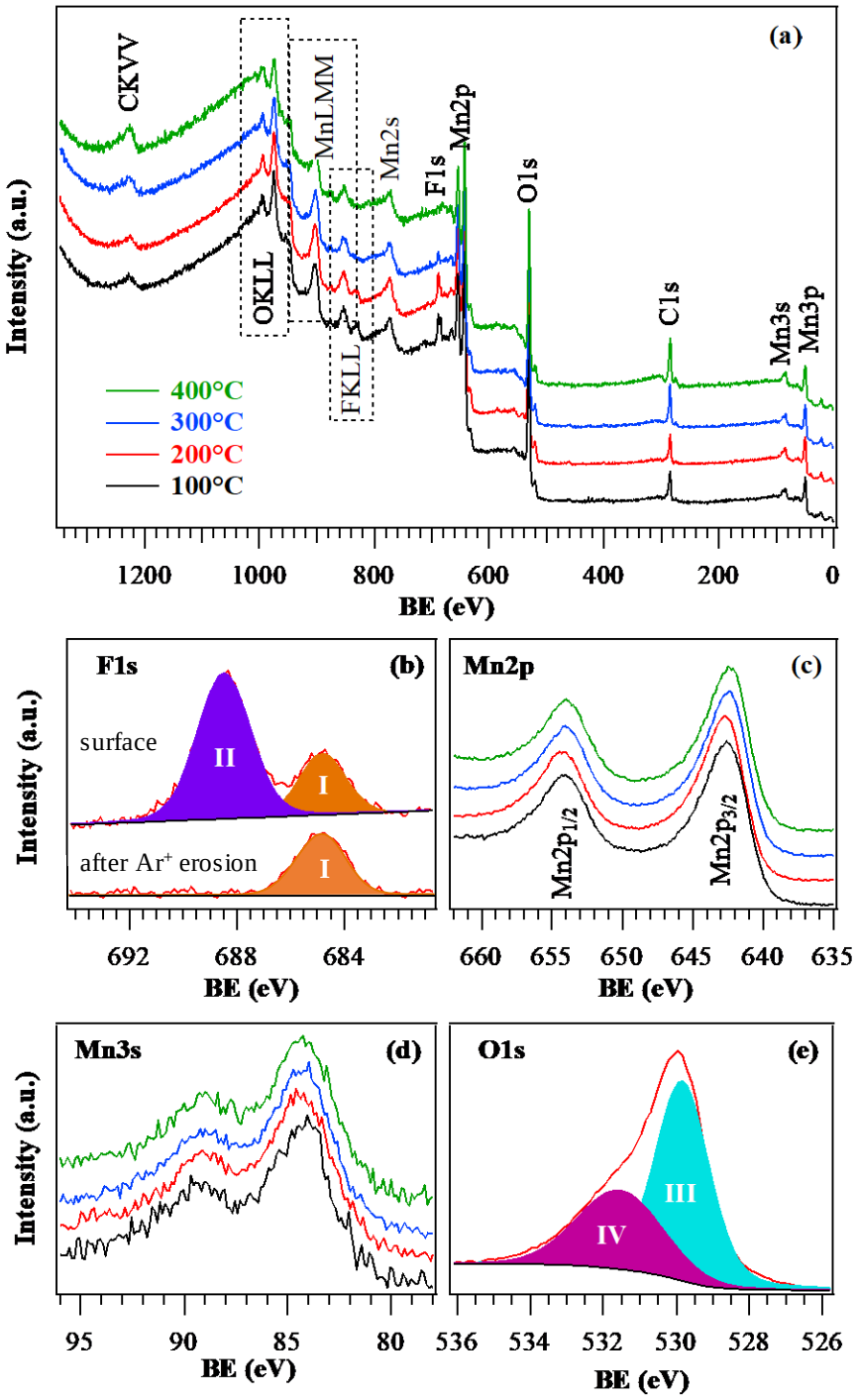

Figure S1. XPS analysis of manganese oxide systems grown on Si(100) substrates at different temperatures: (a) wide-scan spectra; (b) F1s photopeaks for a specimen fabricated at 200°C, along with the corresponding fitting components, before and after 10 min of Ar^+ erosion; (c)-(d) Mn2p and Mn3s photopeaks; (e) O1s signal for a sample grown at 200°C, along with the fitting components.

The O1s photoelectron peak (Figure S1e) could be decomposed by means of two bands, ascribed to different surface oxygen species. The lower BE peak (III, 529.8 eV) was assigned to lattice oxygen in MnO_2, whereas the higher BE one (IV, 531.6 eV) was attributed to both hydroxyl groups and atmospheric oxygen chemisorbed on surface O vacancies.[1-7]

§ S-1.2 X-ray diffraction (XRD)

The average crystallite sizes *D* were estimated from the patterns presented in Figure 2a by using the Scherrer formula:[8-14]

$$D = 0.9[\lambda/(FWHM*\cos\theta)] \quad (S1)$$

where λ, 2θ and FWHM denote respectively the X-ray source excitation wavelength (0.15418 nm), the angular position and the full width at half maximum of the observed diffraction peaks. In this work, the calculation was performed on the (101) reflection.[15] From the same reflection, microstrain (ε) and dislocation density (δ) values were estimated through the following equations:[8,16-17]

$$\varepsilon = FWHM/(4*\mathrm{tg}\theta) \quad (S2)$$

$$\delta = 1/D^2 \quad (S3)$$

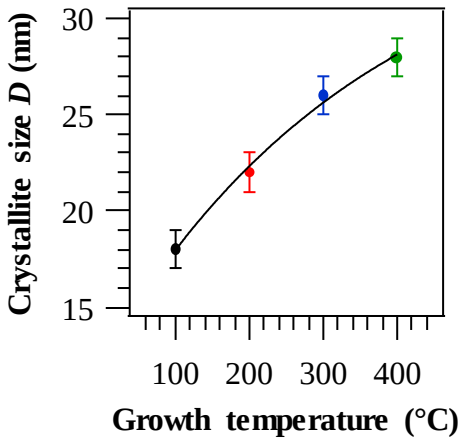

Figure S2. Dependence of the average nanocrystal size, calculated by XRD data, on the deposition temperature for MnO_2 nanosystems.

§ S-1.3 Energy dispersive X-ray spectroscopy (EDXS)

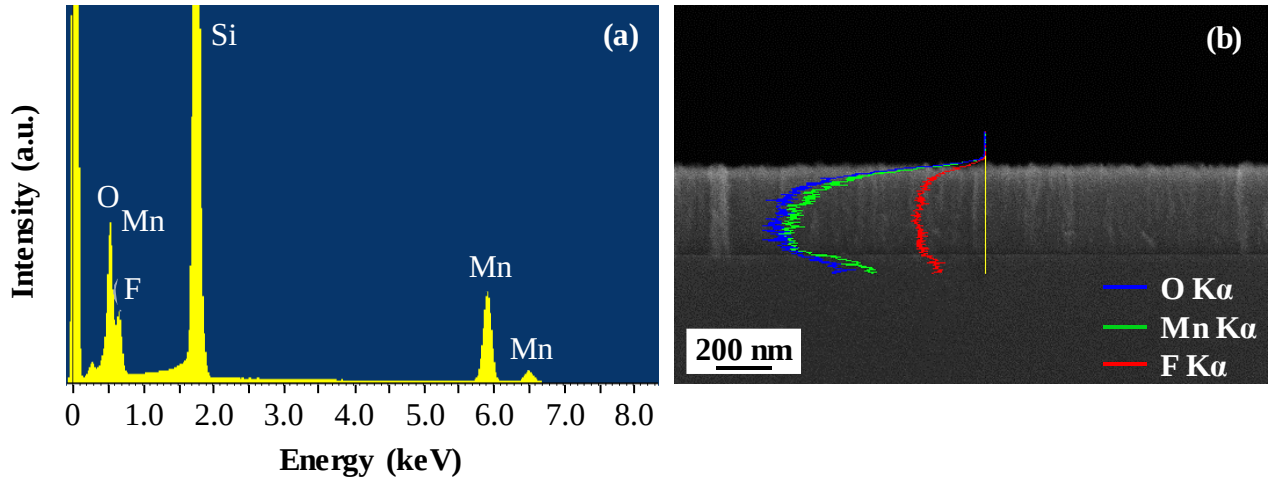

Figure S3. EDXS spectrum (a) and cross-sectional EDXS line scan data (b) for a MnO_2 sample deposited at 100°C.

§ S-1.4 Atomic force microscopy (AFM)

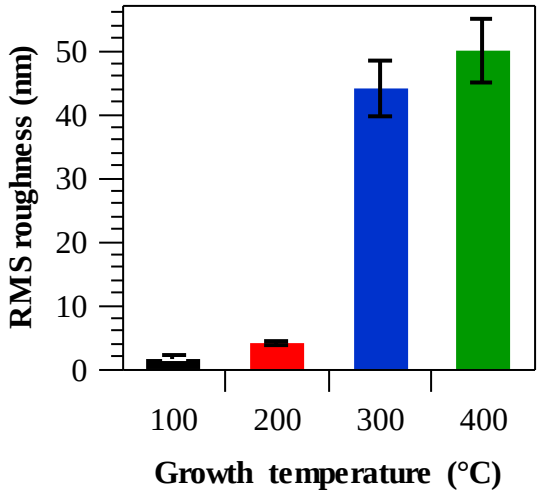

Figure S4. Root-mean-square (RMS) roughness estimated by AFM analyses as a function of the growth temperature for manganese dioxide samples.

References

(1) Yan, D.; Yan, P. X.; Cheng, S.; Chen, J. T.; Zhuo, R. F.; Feng, J. J.; Zhang, G. A. Fabrication, In-Depth Characterization, and Formation Mechanism of Crystalline Porous Birnessite MnO_2 Film with Amorphous Bottom Layers by Hydrothermal Method. *Cryst. Growth Des.* **2009**, *9*, 218-222.

(2) Li, Y.; Li, Y. P.; Wan, Y.; Zhan, S. H.; Guan, Q. X.; Tian, Y. Structure-Performance Relationships of MnO_2 Nanocatalyst for the Low-Temperature SCR Removal of NO_X under Ammonia. *RSC Adv.* **2016**, *6*, 54926-54937.

(3) Gao, J. J.; Jia, C. M.; Zhang, L. P.; Wang, H. M.; Yang, Y. H.; Hung, S. F.; Hsu, Y. Y.; Liu, B. Tuning Chemical Bonding of MnO_2 through Transition-Metal Doping for Enhanced CO Oxidation. *J. Catal.* **2016**, *341*, 82-90.

(4) Xu, H.; Qu, Z.; Zhao, S.; Mei, J.; Quan, F.; Yan, N. Different Crystal-Forms of One-Dimensional MnO_2 Nanomaterials for the Catalytic Oxidation and Adsorption of Elemental Mercury. *J. Hazard. Mater.* **2015**, *299*, 86-93.

(5) Hu, P. P.; Huang, Z. W.; Hua, W. M.; Gu, X.; Tang, X. F. Effect of H_2O on Catalytic Performance of Manganese Oxides in NO Reduction by NH_3. *Appl. Catal., A* **2012**, *437*, 139-148.

(6) Ma, Y. Y.; Wang, R. F.; Wang, H.; Key, J. L.; Ji, S. Control of MnO_2 Nanocrystal Shape from Tremella to Nanobelt for Ehancement of the Oxygen Reduction Reaction Activity. *J. Power Sources* **2015**, *280*, 526-532.

(7) Huang, Z.-H.; Song, Y.; Feng, D.-Y.; Sun, Z.; Sun, X.; Liu, X.-X. High Mass Loading MnO_2 with Hierarchical Nanostructures for Supercapacitors. *ACS Nano* **2018**, *12*, 3557-3567.

(8) Ramesh, M.; Nagaraja, H. S.; Rao, M. P.; Anandan, S.; Huang, N. M. Fabrication, Characterization and Catalytic Activity of α-MnO_2 Nanowires for Dye Degradation of Reactive Black 5. *Mater. Lett.* **2016**, *172*, 85-89.

(9) Haddad, N.; Ben Ayadi, Z.; Mahdhi, H.; Djessas, K. Influence of Fluorine Doping on the Microstructure, Optical and Electrical Properties of SnO_2 Nanoparticles. *J. Mater. Sci. Mater. Electron.* **2017**, *28*, 15457-15465.

(10) Balamurugan, S.; Rajalakshmi, A.; Balamurugan, D. Acetaldehyde Sensing Property of Spray Deposited β-MnO_2 Thin Films. *J. Alloys Compd.* **2015**, *650*, 863-870.

(11) Toufiq, A. M.; Wang, F. P.; Javed, Q. U.; Li, Q. S.; Li, Y. Hydrothermal Synthesis of MnO_2 Nanowires: Structural Characterizations, Optical and Magnetic Properties. *Appl. Phys. A* **2014**, *116*, 1127-1132.

(12) Vijayalakshmi, K.; Renitta, A.; Jereil, S. D.; Alagusundaram, K. Highly (101) Oriented MnO_2 Nanofibers Synthesized using Novel Spray Pyrolysis Technique. *J. Mater. Sci. Mater. Electron.* **2015**, *26*, 9782-9788.

(13) Tawil, S. N. M.; Norhidayah, C. A.; Sarip, N.; Kamaruddin, S. A.; Nurulfadzilah, A. R.; Miskon, A.; Sahdan, M. Z. Effect of Rare-Earth Gd Incorporation on the Characteristics of ZnO Thin Film. *J. Nanosci. Nanotechnol.* **2015**, *15*, 9212-9216.

(14) Shang, J.; Xie, B.; Li, Y.; Wei, X.; Du, N.; Li, H.; Hou, W.; Zhang, R. Inflating Strategy to Form Ultrathin Hollow MnO_2 Nanoballoons. *ACS Nano* **2016**, *10*, 5916-5921.

(15) Pattern No. 024-0735, JCPDS (2000).

(16) Aydogu, S.; Coban, M. B.; Cabuk, G. Influence of Doping Fluorine on the Structural, Surface Morphological and Optical Properties of CdO Films. *Appl. Phys. A* **2017**, *123*, 409.

(17) Bigiani, L.; Barreca, D.; Gasparotto, A.; Sada, C.; Marti-Sanchez, S.; Arbiol, J.; Maccato, C. Controllable Vapor Phase Fabrication of F:Mn_3O_4 Thin Films Functionalized with Ag and TiO_2. *CrystEngComm* **2018**, *20*, 3016-3024.